Published in Journal of Molecular Catalysis A: Chemical 219, issue 2, 255-264, 2004
which should be used for any reference to this work

Oxidation of alkanes with *m*-chloroperbenzoic acid catalyzed by iron(III) chloride and a polydentate amine

Georgiy B. Shul'pin [a,*], Helen Stoeckli-Evans [b], Dalmo Mandelli [c], Yuriy N. Kozlov [a], Ana Tesouro Vallina [b], Camile B. Woitiski [c], Ricardo S. Jimenez [c], Wagner A. Carvalho [c]

[a] *Semenov Institute of Chemical Physics, Russian Academy of Sciences, Ulitsa Kosygina, Dom 4, Moscow 119991, Russia*
[b] *Institut de Chimie, Université de Neuchâtel, Avenue de Bellevaux 51, Case Postale 2, CH-2007 Neuchâtel, Switzerland*
[c] *Instituto de Química, Universidade Estadual de Campinas, P.O. Box 6154, 13083-970 Campinas, SP, Brazil*

Abstract

Tetradentate amine *N*,*N*′-bis(2-pyridylmethylene)-1,4-diaminodiphenyl ether (compound **1**) dramatically accelerates the oxidation of alkanes with MCPBA in acetonitrile catalyzed by $FeCl_3$, whereas *N*,*N*′-bis(2-pyrrolidinmethylene)-1,4-diaminodiphenyl ether (**2**) does not affect the reaction. The selectivity of the reaction in the presence of **1** is noticeably higher than that in its absence. On the basis of the kinetic study and selectivity parameters a mechanism has been proposed which includes the formation of a complex between a molecule of MCPBA and coordinated to ligand **1** iron ion. This complex decomposes to produce a Fe(II) derivative which is further oxidized by MCPBA to generate a $(\mathbf{1}\cdot Fe{=}O)^{4+}$ species reacting with both alkane and acetonitrile. Finally, alkyl hydroperoxide is formed which partially decomposes to produce more stable corresponding alcohol and ketone (aldehyde).

Keywords: Alkanes; Biomimetics; Iron complexes; Ligand effects; *meta*-Chloroperbenzoic acid (MCPBA)

1. Introduction

Oxygen-activating proteins and especially enzymes containing non-heme iron sites (for example, methane monooxygenase, MMO) [1–15] can be mimicked by synthesized non-heme iron complexes with polydentate nitrogen-containing ligands [16–32]. In some cases in these alkane-oxidizing systems *m*-chloroperoxybenzoic acid (MCPBA) was used as an oxidant [33,34]. Complexes of cobalt [34], ruthenium [35–37] and manganese [34,38,39] with chelating *N*-ligands have been also found to catalyze alkane oxidations with MCPBA. It is well-known that alkane oxidations with various reagents catalyzed by "simple" transition metal salts can be dramatically accelerated if certain additives are introduced into the reaction solution (see reviews [40,41]). These additives are often amines or their derivatives which can be considered as models of protein environment of enzyme active sites.

We wish report a new catalytic system based on iron(III) chloride as a catalyst and MCPBA as an oxidizing reagent. We studied the effect of the addition of tetradentate amines **1** and **2** and found that only compound **1** gives rise to the remarkable growth of the reaction rate as well as to noticeably higher regio- and bond-selectivity in the alkane oxidation. Polydentate *N*-ligands can be considered as models of amino acid environment of certain enzyme reaction centers.

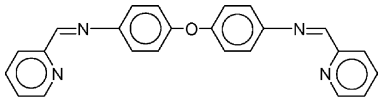

1

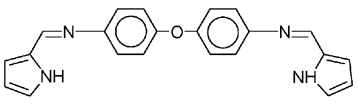

2

* Corresponding author. Tel.: +7 095 939 7317; fax: +7 095 137 6130.
E-mail address: shulpin@chph.ras.ru (G.B. Shul'pin).

2. Experimental

2.1. Materials and instruments

All chemicals employed were commercially available reagent grade materials from Aldrich Chemicals Co. and Fluka Chemie AG and were used as received, without further purification.

IR spectra were obtained on a Perkin-Elmer FT-IR 1720X spectrometer using KBr pellets. The abbreviations for the described intensities are: b (broad), w (weak), m (medium), s (strong) and vs (very strong). The absorption bands are given in cm^{-1} and the spectrum was taken in the range between 4000 and 400 cm^{-1}. The NMR spectrum was recorded on a BRUKER AMX-400 (400 MHz) spectrometer. Chemical shifts (δ) are reported in ppm values relative to TMS. The abbreviations used are: s (singlet), d (doublet), t (triplet), m (multiplet) and b (broad). The electron impact (EI) mass spectrum was obtained using a DELSI-NERMAG R30-10 system. The electrospray (ESI) mass spectrum was performed by the MS-Service UNI Fribourg using a BRUKER FTMS 4.7T BioAPEX II system. UV-Vis titration measurements were performed in 96-well microtitre plates monitored in a Spectramax-250 plate reader at the Department of Chemistry and Biochemistry of the University of Bern. The results were analyzed using SoftmaxPro 2.2.1 and then treated with Excel2000 Worksheets.

In the X-ray analysis, intensity data were measured either on a STOE AED2 four-circle diffractometer or on a STOE Imaging Plate diffractometer both using graphite monochromated Mo Ka radiation ($l = 0.71073$). The structures were solved either by direct methods or by Patterson heavy-atom technique using the program SHELXS-97 [42]. The program SHELXL-97 [43] was used for refinement. The H atoms were included at calculated positions and allowed to ride on their parent atoms with $U\text{iso} = xU_{\text{eq}}$ (parent), where $x = 1.5$ for methyl H atoms and $x = 1.2$ for all other atoms. Weighted full-matrix least squares refinement on F^2 was used. Neutral atomic scattering factors are taken from International Tables for X-ray crystallography [44].

The values $R1$ and $wR2$ given in the tables have been calculated as follows:

$$R1 = \frac{\sum ||F_o| - |F_c||}{\sum |F_o|}$$

$$wR2 = \sqrt{\frac{\sum w(F_o^2 - F_c^2)^2}{\sum (wF_o^4)}}$$

with

$$w = \frac{1}{[\sigma^2(F_o^2) + (AP)^2 + BP]}; \qquad P = \frac{(F_o^2 + 2F_c^2)}{3}$$

The goodness of fit ratio is given by

$$\text{GoF} = \sqrt{\frac{\sum w(F_o - F_c)^2}{n - p}}$$

with n = number of reflections, p = number of refined parameters.

The figures were drawn using the program PLUTON/PLATON [45]. Thermal ellipsoids are at the 50% probability level.

*2.2. N,N′-bis(2-pyridylmethylene)-1,4-diaminodiphenyl ether (compound **1**)*

Compound **1** [46] was prepared by the condensation reaction between 4,4′-diaminophenyl ether and pyridine-2-carboxaldehyde in a 1:2 ratio with a quantitative yield. To a solution of tetrahydrofurane (50 mL) containing 4,4′-diaminophenyl ether (10.465 mmol, 2.096 g), was added drop-by-drop pyridine-2-carboyaldehyde (20.930 mmol, 2 mL). The mixture was heated at reflux, with stirring, for 6 h. Removal of solvent under vacuum yielded **1** as a yellow powder which was dried under high vacuum for several hours (yield: 3.87 g, 98.0%). Suitable crystals for crystallographic analysis were obtained by slow diffusion of hexane into a solution of the ligand in dichloromethane. ^{1}H NMR (CD_3OD, 400 MHz, ppm): 8.70 [ddd, Ha, $^3J(a,b) = 4.9$, $^4J(a,c) = 1.7$, $^5J(a,d) = 0.9$, 2H], 8.66 (s, imine, 2H), 8.24 (td, Hd, $^3J(d,c) = 7.9$, $^4J(d,b) = 1.2$, $^5J(d,a) = 0.9$, 2H], 8.00 [ddt, Hc, $^3J(c,d) = 7.9$, $^4J(c,b) = 7.5$, $^5J(c,a) = 1.7$, 2H], 7.54 [ddd, Hb, $^3J(b,c) = 7.5$, $^4J(b,a) = 4.9$, $^5J(b,d) = 1.2$, 2H], 7.43 [td, Hf, $3J(f,g) = 8.9$, $^5J(f,e) =$

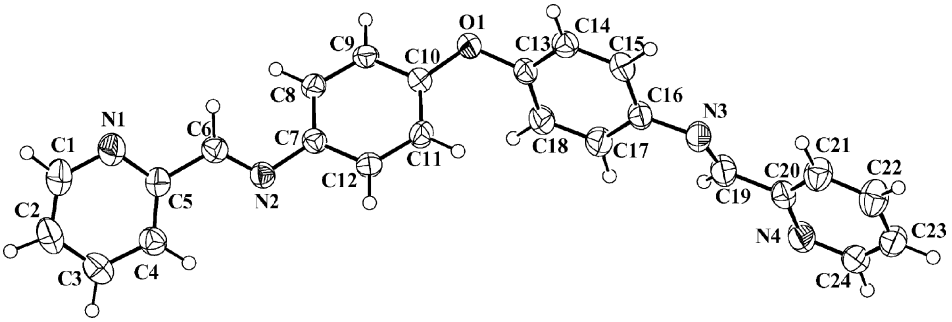

Fig. 1. Molecular structure of compound **1**.

Table 1
Crystal data for compound **1**

$C_{24}H_{18}N_4O$	Mo Ka radiation $l = 0.71073$ Å	
$M_r = 378.4$	Cell parameters from 5000 reflections	
Monoclinic	$1.99 < q < 25.89$	
P 2_1/c (No. 14)	$D_x = 1.337\,g\,cm^{-3}$	
$a = 12.340(1)$ Å	$\alpha = 90^\circ$	$\mu = 0.08\,mm^{-1}$
$b = 18.385(2)$ Å	$\beta = 91.96(1)^\circ$	$T = 153\,K$
$c = 8.587(1)$ Å	$\gamma = 90^\circ$	Block
$V = 1947.0(3)$ Å^3	0.55 mm × 0.50 mm × 0.35 mm	
Z = 4	Yellow	
Data collection		
STOE IPDS diffractometer	Rint = 0.0323	
Profile data from phi oscillation scans	$\theta_{max} = 25.89^\circ$	
14238 measured reflections	$h = -14 \rightarrow 15$	
3716 independent reflections	$k = -22 \rightarrow 22$	
2904 observed reflections [$I > 2\sigma(I)$]	$l = -10 \rightarrow 10$	
Refinement		
Refinement on F^2	$(\Delta/\sigma)_{max} = 0.00$	
[$I > 2\sigma(I)$] $R1 = 0.0347$ $wR2 = 0.0896$	$\Delta\rho_{max} = 0.15\,e\,Å^{-3}$	
GoF = 1.015	$\Delta\rho_{min} = -0.13\,e\,Å^{-3}$	
334 parameters refined		
Structure Solving Program: SHELXS-97, Structure Refinement Program: SHELXL-97		

2.7, 4H], 7.14 [td, Hg, $^3J(g, f) = 8.9$, $^5J(g, e) = 2.7$, 4H]. ^{13}C NMR (CD_3OD, 400 MHz, ppm): 159.27, 156.92, 154.46, 149.57, 146.49, 137.78, 125.87, 122.97, 122.38, 119.62. IR (KBr pellet, cm^{-1}): 3047 (w), 2905 (w), 1624 (s), 1581 (s), 1566 (m), 1495 (vs), 1467 (m), 1433 (m), 1344 (w), 1240 (vs), 1198 (s), 993 (m), 859 (s), 832 (s), 776 (s), 542 (m). MS (EI, 70 eV), *m/z* (%): 379 (MH+), 197, 182, 169. Anal. For $C_{24}H_{18}N_4O$ (Mr = 378.43 g mol^{-1}). Calc. (%) C: 76.17 H: 4.80 N: 14.80. Found (%) C: 75.90 H: 4.86 N: 14.83.

Table 2
Atomic coordinates (× 10^4) and equivalent isotropic displacement parameters U_{eq} (Å^2 × 10^3) for compound **1**

	x	*y*	*z*	U_{eq}
N(1)	1949(1)	1832(1)	−2525(2)	59(1)
N(2)	4239(1)	1186(1)	−315(1)	35(1)
N(3)	8963(1)	−453(1)	8514(1)	44(1)
N(4)	11556(1)	−1273(1)	8390(1)	53(1)
O(1)	6241(1)	1582(1)	5556(1)	42(1)
C(1)	1526(1)	1843(1)	−3984(2)	68(1)
C(2)	2005(1)	1530(1)	−5238(2)	59(1)
C(3)	2980(1)	1179(1)	−4996(2)	51(1)
C(4)	3438(1)	1157(1)	−3508(2)	42(1)
C(5)	2898(1)	1484(1)	−2303(1)	38(1)
C(6)	3359(1)	1506(1)	−698(2)	39(1)
C(7)	4710(1)	1286(1)	1199(1)	33(1)
C(8)	4742(1)	1963(1)	1944(1)	35(1)
C(9)	5281(1)	2047(1)	3369(1)	35(1)
C(10)	5770(1)	1453(1)	4099(1)	33(1)
C(11)	5744(1)	777(1)	3377(2)	39(1)
C(12)	5239(1)	703(1)	1923(2)	37(1)
C(13)	6938(1)	1063(1)	6226(1)	36(1)
C(14)	6689(1)	792(1)	7664(2)	39(1)
C(15)	7385(1)	296(1)	8396(2)	39(1)
C(16)	8329(1)	78(1)	7704(1)	39(1)
C(17)	8563(1)	362(1)	6248(2)	48(1)
C(18)	7872(1)	854(1)	5505(2)	46(1)
C(19)	9934(1)	−568(1)	8194(2)	48(1)
C(20)	10584(1)	−1138(1)	8989(2)	41(1)
C(21)	10215(1)	−1501(1)	10273(2)	51(1)
C(22)	10861(1)	−2025(1)	10971(2)	58(1)
C(23)	11860(1)	−2166(1)	10372(2)	52(1)
C(24)	12169(1)	−1780(1)	9086(2)	52(1)

According to the X-ray analysis (Tables 1–5), compound **1** has an imine *E* configuration. The molecule possesses *pseudo*-C_2 symmetry with the twofold axis running through the central O atom. The conformation of the two halves of the molecule is quite different. One moiety, to the right in Fig. 1, is almost flat with a dihedral angle of 10.77(8)° between the phenyl and the pyridine rings. In the second half of the molecule the rings are inclined to one another by 46.35(5)°. The pyridine-imine system is almost planar within the two moieties. Torsion angles N1-C5-C6-N2 and C7-N2-C6-C5 are 178.3(1) and 173.3(1)°, respectively, whereas torsion angles N3-C19-C20-N4 and C16-N3-C19-C20 are 170.0(1) and -177.7(1)°, respectively. This is consistent with the presence of a π-system, only interrupted by the central O atom, although bond-length alternation is always observed (the average C=N bond distance of 1.263(1)° is indicative of double-bond character). In the crystal packing (Fig. 2) it can be seen that the pyridine N atoms are involved in weak intermolecular C–H · · · N interactions with symmetry-related molecules.

2.3. N,N′-bis(2-pyrrolidinmethylene)-1,4-diaminodiphenyl ether (2)

Compound **2** was obtained by the condensation reaction between 4,4′-diaminophenyl ether and pyrrol-2-carboxaldehyde in a 1:2 ratio with a high yield. To a solution of THF (10 mL) containing 4,4′-diaminophenyl ether

Table 3
Selected bond distances [Å] for compound **1**

N(1)–C(1)	1.341(2)
N(1)–C(5)	1.3418(16)
N(2)–C(6)	1.2698(15)
N(2)–C(7)	1.4167(15)
N(3)–C(19)	1.2564(17)
N(3)–C(16)	1.4179(15)
N(4)–C(24)	1.3302(18)
N(4)–C(20)	1.3445(16)
O(1)–C(10)	1.3817(14)
O(1)–C(13)	1.3963(13)
C(1)–C(2)	1.372(2)
C(1)–H(1)	0.96(2)
C(2)–C(3)	1.375(2)
C(2)–H(2)	0.965(17)
C(3)–C(4)	1.3800(19)
C(3)–H(3)	0.995(18)
C(4)–C(5)	1.3874(18)
C(4)–H(4)	1.003(16)
C(5)–C(6)	1.4734(17)
C(6)–H(6)	0.996(15)
C(7)–C(12)	1.3908(16)
C(7)–C(8)	1.4002(16)
C(8)–C(9)	1.3811(17)
C(8)–H(8)	0.981(14)
C(9)–C(10)	1.3869(16)
C(10)–C(11)	1.3885(16)
C(11)–C(12)	1.3830(17)
C(11)–H(11)	0.941(14)
C(12)–H(12)	0.953(14)
C(13)–C(14)	1.3760(18)
C(13)–C(18)	1.3816(18)
C(14)–C(15)	1.3882(17)
C(14)–H(14)	0.961(15)
C(15)–C(16)	1.3857(17)
C(15)–H(15)	0.955(15)
C(16)–C(17)	1.3943(19)
C(17)–C(18)	1.3827(18)
C(17)–H(17)	0.984(16)
C(18)–H(18)	0.966(17)
C(19)–C(20)	1.4731(18)
C(19)–H(19)	1.02(2)
C(20)–C(21)	1.3793(19)
C(21)–C(22)	1.375(2)
C(21)–H(21)	1.010(16)
C(22)–C(23)	1.376(2)
C(22)–H(22)	0.932(19)
C(23)–C(24)	1.377(2)
C(23)–H(23)	0.974(16)
C(24)–H(24)	0.973(16)
C(9)–H(9)	0.954(13)

(2.5 mmol, 0.500 g), was added drop by drop a solution of pyrrol-2-carboyaldehyde (5 mmol, 0.475 g) in THF (15 mL). The mixture was heated at reflux under N_2 atmosphere with stirring, for 8 h. Removal of solvent under vacuum yielded **2** as yellow powder that was washed with THF and dried afterwards under high vacuum for several hours to afford 0.75 g (yield: 86.0%). ^{1}H NMR (DMSO-d_6, 400 MHz, ppm): 11.74 (b, 2H, NH), 8.33 (s, 2H, imine), 7.24 [td, ph, $^3J(a, b) = 8.8$, $^3J(a, d) = 3.3$, $^4J(a, c) = 2.1$, 4H], 7.04 (m, 6H, Hc and ph), 6.69 (m, 2H, Ha), 6.21 (s, 2H, Hb). ^{13}C

Table 4
Selected bond angles (°) for compound **1**

C(1)–N(1)–C(5)	116.74(13)
C(6)–N(2)–C(7)	119.80(10)
C(19)–N(3)–C(16)	121.48(12)
C(24)–N(4)–C(20)	117.26(12)
C(10)–O(1)–C(13)	119.39(9)
N(1)–C(1)–C(2)	124.25(15)
N(1)–C(1)–H(1)	114.6(12)
C(2)–C(1)–H(1)	121.2(12)
C(1)–C(2)–C(3)	118.42(14)
C(1)–C(2)–H(2)	118.2(10)
C(3)–C(2)–H(2)	123.4(10)
C(2)–C(3)–C(4)	118.86(14)
C(2)–C(3)–H(3)	119.1(10)
C(4)–C(3)–H(3)	122.1(10)
C(3)–C(4)–C(5)	119.07(12)
C(3)–C(4)–H(4)	121.6(9)
C(5)–C(4)–H(4)	119.3(9)
N(1)–C(5)–C(4)	122.66(12)
N(1)–C(5)–C(6)	115.25(11)
C(4)–C(5)–C(6)	122.02(11)
N(2)–C(6)–C(5)	121.93(11)
N(2)–C(6)–H(6)	122.2(8)
C(5)–C(6)–H(6)	115.9(8)
C(12)–C(7)–C(8)	118.35(10)
C(12)–C(7)–N(2)	118.77(10)
C(8)–C(7)–N(2)	122.66(10)
C(9)–C(8)–C(7)	120.63(10)
C(9)–C(8)–H(8)	119.3(8)
C(7)–C(8)–H(8)	120.0(8)
C(8)–C(9)–C(10)	120.09(10)
C(8)–C(9)–H(9)	120.8(8)
C(10)–C(9)–H(9)	119.1(8)
O(1)–C(10)–C(9)	115.93(10)
O(1)–C(10)–C(11)	124.02(10)
C(9)–C(10)–C(11)	120.03(11)
C(12)–C(11)–C(10)	119.55(11)
C(12)–C(11)–H(11)	120.2(8)
C(10)–C(11)–H(11)	120.2(8)
C(11)–C(12)–C(7)	121.25(11)
C(14)–C(13)–C(18)	121.16(11)
C(14)–C(13)–O(1)	117.61(11)
C(18)–C(13)–O(1)	121.17(11)
C(13)–C(14)–C(15)	119.34(12)
C(13)–C(14)–H(14)	120.7(9)
C(15)–C(14)–H(14)	120.0(9)
C(16)–C(15)–C(14)	120.82(12)
C(16)–C(15)–H(15)	119.1(8)
C(14)–C(15)–H(15)	120.1(8)
C(15)–C(16)–C(17)	118.58(11)
C(15)–C(16)–N(3)	116.52(11)
C(17)–C(16)–N(3)	124.81(11)
C(18)–C(17)–C(16)	121.09(12)
C(18)–C(17)–H(17)	117.5(9)
C(16)–C(17)–H(17)	121.4(9)
C(13)–C(18)–C(17)	119.01(12)
C(13)–C(18)–H(18)	120.0(9)
C(17)–C(18)–H(18)	121.0(9)
N(3)–C(19)–C(20)	121.79(13)
N(3)–C(19)–H(19)	121.2(10)
C(20)–C(19)–H(19)	117.0(10)
N(4)–C(20)–C(21)	122.68(12)
N(4)–C(20)–C(19)	115.63(12)
C(21)–C(20)–C(19)	121.68(12)
C(22)–C(21)–C(20)	119.03(13)

Table 4 (*Continued*)

C(22)–C(21)–H(21)	121.6(9)
C(20)–C(21)–H(21)	119.3(9)
C(21)–C(22)–C(23)	118.87(15)
C(21)–C(22)–H(22)	122.6(11)
C(23)–C(22)–H(22)	118.4(11)
C(22)–C(23)–C(24)	118.56(13)
C(22)–C(23)–H(23)	120.4(9)
C(24)–C(23)–H(23)	121.0(9)
N(4)–C(24)–C(23)	123.59(13)
N(4)–C(24)–H(24)	115.3(9)
C(23)–C(24)–H(24)	121.1(9)
C(11)–C(12)–H(12)	120.7(8)
C(7)–C(12)–H(12)	118.1(8)

NMR (DMSO-d_6, 400 MHz, ppm): 155.25, 150.79, 148.42, 131.47, 124.60, 123.10, 120.10, 117.14, 110.55. IR (KBr pellet, cm^{-1}): 3413 (vs), 2959 (w), 2889 (w), 1617 (vs), 1549 (w), 1499 (vs), 1452 (m), 1421 (s), 1332 (w), 1282 (m), 1260 (s), 1240 (m), 1196 (s), 1082 (s), 1008 (w), 882 (m), 836 (vs), 728 (vs), 666 (m), 532 (m). MS (ESI, *m/z*), *m/z*: 355 (MH^+), 278, 211. Anal. For $C_{22}H_{18}N_4O{\cdot}H_2O$ (Mr = 360.41 g mol^{-1}). Calc. (%): C: 73.32 H: 5.22 N: 15.54. Found (%): C: 73.50 H: 5.46 N: 14.76.

The IR spectrum of **2** exhibits a very strong peak at 3413 cm^{-1} that corresponds to the free pyrrol NH group vibration and several weak peaks at 3113, 3063, 3032, 2959 and 2889 cm^{-1}, associated with the arC–H stretching vibrations. The imine-stretching band appears at 1617 cm^{-1} as an intense signal and the arC–arC stretching vibrations bands at 1549, 1499, 1452 and 1421 cm^{-1}. The peaks associated with the ether function asymmetric stretching band are found at 1260, 1240 and 1196 cm^{-1}. Bending C–H vibrations appear at 836 and 728 cm^{-1}. The ^1H NMR spectrum exhibits six sets of resonances, five of them in the aromatic region. The proton of the pyrrol NH group is observed at 11.74 ppm. The UV-Vis spectrum (250–600 nm region) of **2** in EtOH at a concentration 125 μmol dm^{-3} shows one clear band at 340 nm with a small shoulder at about 295 nm corresponding to the absorption of the imine chromophore and the diphenyl ether groups.

2.4. Catalytic oxidations

The oxidations of hydrocarbons were carried out in MeCN at 25 °C in air in thermostated Pyrex cylindrical vessels with vigorous stirring. The total volume of the reaction solution was 5 mL. Initially, a portion of solid MCPBA ("Fluka") was added to the solution of the catalyst, co-catalyst and substrate. In the experiments on cyclohexane oxidation after certain time intervals samples (about 0.2 mL) were taken. In order to determine concentrations of all cyclohexane oxidation products the samples of reaction solutions were analyzed twice (before and after their treatment with PPh_3) by GC (HP Series 5890-II, Carbowax 20 M, 25 m × 0.2 mm × 0.2 μm; helium as a carrier gas) measuring concentrations of cyclohexanol and cyclohexanone. This simple and convenient method (an excess of solid triphenylphosphine is added to the samples 10–15 min before the GC analysis) which was described by us earlier [40,41,47–52] allows us to detect alkyl hydroperoxides and to measure also the real concentrations of all three products (alkyl hydroperoxide, alcohol and aldehyde or ketone) present in the reaction solution, because usually alkyl hydroperoxides are decomposed in the gas chromatograph to produce mainly the corresponding alcohol and ketone. Authentic samples of all oxygenated products were used to attribute the peaks in chromatograms

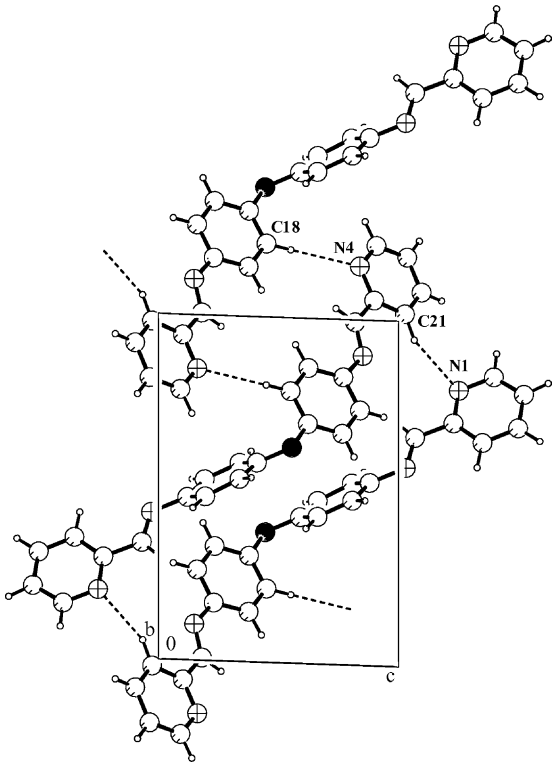

Fig. 2. Crystal packing of compound **1** showing C–H···N interactions as dotted lines.

Table 5
Hydrogen-bonding geometry (Å, °) for compound **1**[a]

	D–H···A	*d*(D–H)	*d*(H···A)	*d*(D···A)	<(DHA)
#1	C(18)–H(18)···N(4)	0.97(2)	2.57(2)	3.526(2)	168(1)
#2	C(21)–H(21)···N(1)	1.01(2)	2.55(2)	3.405(2)	142(1)

#1: $-x+2,-y,-z+1$; #2: $-x+1,-y,-z+1$.

[a] Symmetry transformations used to generate equivalent atoms.

(comparison of retention times was carried out for different regimes of GC-analysis).

3. Results and discussion

The efficiency of the cyclohexane oxidation with MCPBA in acetonitrile at 25 °C catalyzed by only $FeCl_3$ is very low (Fig. 3). However, we have found that addition of a relatively small amount of compound **1** leads to the dramatic increase of both the initial reaction rate and the final yield of cyclohexane oxygenates. It is noteworthy that no oxidation acceleration has been found when compound **2** was used instead of **1**. Thus, in the reaction of cyclohexane (0.4 mol dm^{-3}) oxidation with MCPBA (0.5 mol dm^{-3}) in acetonitrile at 25 °C catalyzed by $FeCl_3$ (2×10^{-4} mol dm^{-3}) and compound **2** (3.2×10^{-3} mol dm^{-3}) we obtained after 90 min (and after the reduction with PPh_3; see Section 2 and the text below) only very low concentrations of cyclohexanol (1.4×10^{-3} mol dm^{-3}) and cyclohexanone (5×10^{-4} mol dm^{-3}) which correspond to TON = 9 (compare with the data presented in Table 6).

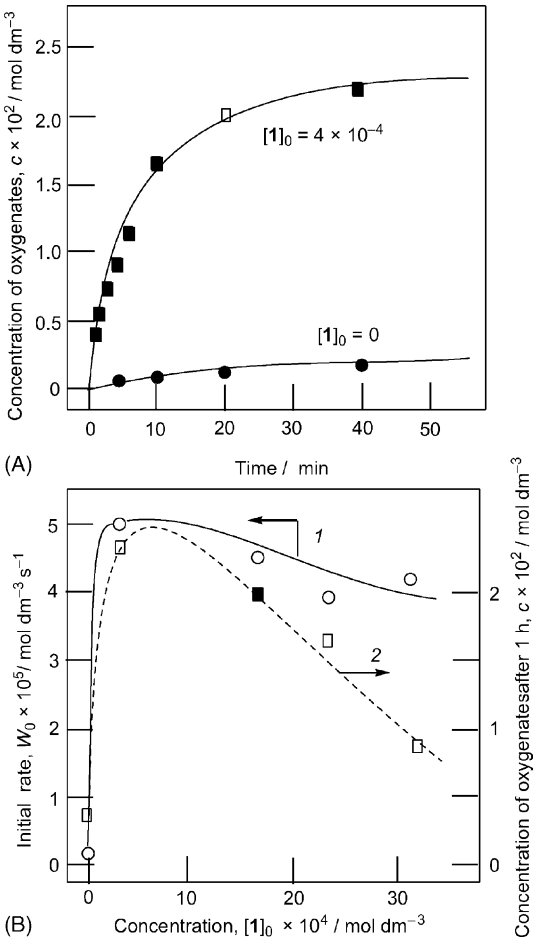

Fig. 3. Cyclohexane (0.4 mol dm^{-3}) oxidation by MCPBA (0.5 mol dm^{-3}) catalyzed by $FeCl_3 \cdot 6H_2O$ (2×10^{-4} mol dm^{-3}) in MeCN at 25 °C. Graph *A*: accumulation of oxygenates with time at two different concentrations of **1** (in mol dm^{-3}). Graph *B*: plots of initial rates of oxygenate accumulation (curve 1) and the total yield of oxygenates after 1 h (curve 2) vs. concentration of added **1**.

Table 6
Cyclohexane oxidation by various systems[a]

Oxidant	System	Products (mol dm^{-3})			TON[b]
		-one	-ol	CyOOH	
MCPBA[c]	$FeCl_3$	0.0004	0.0009	0.0012	12
	$FeCl_3$ + **1**	0.0032	0.0039	0.010	86
	$FeCl_3$ + **2**[d]	0.0005	0.0014		9
	Complex **3**	0.0037	0.0035	0.0025	48
PAA[e]	$FeCl_3$	0.0024	0.0025	0.0037	43
	$FeCl_3$ + **1**	0.0036	0.0065	0.0025	63
	Complex **3**	0.0096	0.0040	0.0130	133

[a] For conditions, see the text.
[b] Number of moles of all products per one mol of Fe.
[c] During 60 min at 25 °C.
[d] After reduction with PPh_3.
[e] During 90 min at 50 °C.

Employing a method previously used by us (a comparison of the chromatograms before and after the reduction with solid triphenylphosphine) [40,41,47–52] we demonstrated that cyclohexyl hydroperoxide is formed in sufficient concentration in addition to the more stable cyclohexanone and cyclohexanol. Nevertheless, in our kinetic studies presented in Figs. 3–6 we measured the concentrations of the cyclohexanone and cyclohexanol only after the reduction with PPh_3 because in this case we obtain more precise values of the initial rates. It can be seen in Fig. 3, graph *B* that at high concentrations of **1** the initial rate does not practically depend on its initial concentration, $[\mathbf{1}]_0$.

Fig. 4 plots the dependence of the initial rate on the concentration of $FeCl_3$, while the concentration of co-catalyst **1** is fixed. The linearity of the slope indicates an order of 1 for $FeCl_3$. We have found a zero-order dependence on initial oxidant concentration (Fig. 5, graph *B*, curve 1). First order has been found for cyclohexane even at its high concentrations (up to 0.8 mol dm^{-3}; Fig. 6).

We can assume that the diphenyl ether bridge that links the two bidentate N_2-units would not permit the ligand to

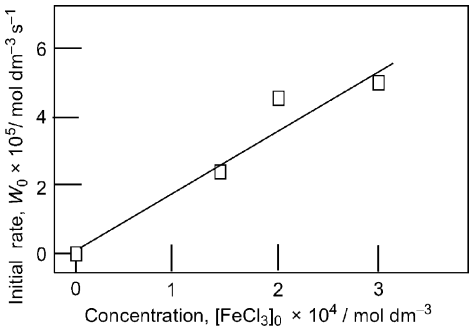

Fig. 4. Dependence of initial oxidation rate on the concentration of $FeCl_3$ in cyclohexane (0.4 mol dm^{-3}) oxidation by MCPBA (0.5 mol dm^{-3}) catalyzed by $FeCl_3 \cdot 6H_2O$ and **1** (16×10^{-4} mol dm^{-3}) in MeCN at 25 °C.

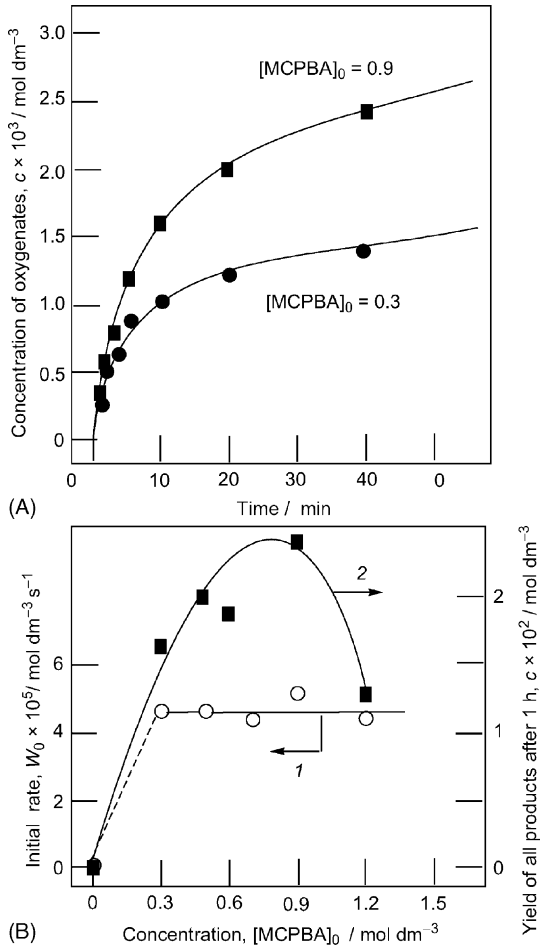

Fig. 5. Cyclohexane (0.4 mol dm^{-3}) oxidation by MCPBA (0.5 mol dm^{-3}) catalyzed by $FeCl_3 \cdot 6H_2O$ (2×10^{-4} mol dm^{-3}) and **1** (16×10^{-4} mol dm^{-3}) in MeCN at 25 °C. Graph *A*: accumulation of oxygenates with time at two different initial concentrations of MCPBA (in mol dm^{-3}). Graph *B*: plots of initial rates of oxygenate accumulation (curve 1) and the total yield of oxygenates after 1 h (curve 2) vs. initial concentration of MCPBA.

wrap around one metal center. As in almost all experiments we used a high **1**:Fe ratio we have to propose that mixing $FeCl_3$ and **1** in acetonitrile solution gives rise to the formation of a complex containing iron(III) ion coordinated with

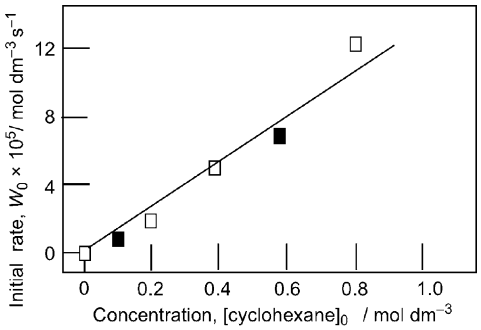

Fig. 6. Dependence of initial oxidation rate on the concentration of cyclohexane in its oxidation by MCPBA (0.5 mol dm^{-3}) catalyzed by $FeCl_3 6H_2O$ (2×10^{-4} mol dm^{-3}) and **1** (16×10^{-4} mol dm^{-3}) in MeCN at 25 °C.

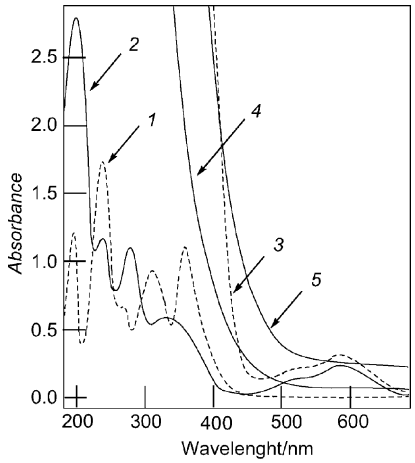

Fig. 7. UV-Vis spectra of $FeCl_3 \cdot 6H_2O$ (2×10^{-4} mol dm^{-3}) (curve 1), complex **3** (4.3×10^{-3} mol dm^{-3}) (curve 2), $FeCl_3 \cdot 6H_2O$ (2×10^{-4} mol dm^{-3}) + **1** (1.6×10^{-3} mol dm^{-3}) (curve 3), the same in the presence of MCPBA (0.5 mol dm^{-3}) after 20 s (curve 4) and 20 min (curve 5). Solvent acetonitrile, 25 °C.

only two nitrogen atoms of compound **1**. It is important to note that a coordination of such type is impossible in the case of compound **2** containing N–H fragments. An independent preliminary experiment supports this assumption: using the relatively low **1**:Fe ratio we were able to isolate an iron complex (**3**) which according to the elemental analysis had the composition $[Fe_2(\mathbf{1})_3](ClO_4)_4$. Compound **3** and the $FeCl_3$ + **1** combination exhibited similar electronic spectra in the region 450–700 nm (Fig. 7). Both complex **3** and the $FeCl_3$ + **1** combination catalyze the cyclohexane oxidation by MCPBA (as well as by peroxyacetic acid, PAA) (see Table 6).

Thus, discussing a possible mechanism of the alkane oxidation we accept that equilibrium (1) exists in the reaction solution, and the formation of an adduct between the iron ion and **1** with the 1:1 ratio is probable

$$Fe^{3+} + \mathbf{1} \rightleftharpoons (Fe \cdot \mathbf{1})^{3+} \quad K_1 \qquad (1)$$

In this case the oxidation rate will be changed with growth of $[\mathbf{1}]_0$ (see Fig. 3, curve 1) until the point when all iron will be involved into a 1:1 complex and this rate will remain almost constant during further growth of $[\mathbf{1}]_0$. The dependence of the initial reaction rate on $[\mathbf{1}]_0$ shown in Fig. 3, curve 1 is in agreement with this proposal. Constant for equilibrium (1) is

$$K_1 = \frac{[(Fe \cdot \mathbf{1})^{3+}]_{equil}}{[Fe^{3+}]_{equil}[\mathbf{1}]_{equil}}$$

At $[\mathbf{1}]_0/[Fe^{3+}]_0 = 1$–2 and $[Fe^{3+}]_0 = 2 \times 10^{-4}$ mol dm^{-3} the reaction rate attains its maximum value, i.e. $[Fe^{3+}]_{equil}/[Fe^{3+}]_0 \geq 0.9$, $[Fe^{3+}]_{equil} < 0.1[Fe^{3+}]_0$ and $[\mathbf{1}]_{equil} \approx [Fe^{3+}]_0$. Thus, using the data presented in Fig. 3 we can estimate $K_1 > 5 \times 10^4$ mol^{-1} dm^3.

We measured the selectivity parameters for the oxidation of certain alkanes by the system under investigation. It can

Table 7
Selectivity parameters in alkane oxidations by various systems in acetonitrile (note that some known systems are added to compare), **1**:Fe = 8:1

Substrate	System	Selectivity[a]
		C(1):C(2):C(3):C(4)
n-Heptane	*m*-CPBA–$FeCl_3$	1:7:6:6
	m-CPBA–$FeCl_3$–**1**	1:29:30:27
	m-CPBA–complex **3**	1:20:22:21
	H_2O_2–*n*-Bu_4NVO_3–PCA[b]	1:6:6:5
	H_2O_2–Mn_2^{IV}–MeCOOH[c]	1:46:35:34
		1°:**2**°:**3**°
Methylcyclohexane	*m*-CPBA–$FeCl_3$	1:14:148
	m-CPBA–$FeCl_3$–**1**	1:21:211
	m-CPBA–complex **3**	1:11:190
	H_2O_2–*n*-Bu_4NVO_3–PCA[b]	1:6:18
	H_2O_2–Mn_2^{IV}–MeCOOH[c]	1:26:200

[a] Parameter C(1):C(2):C(3):C(4) is normalized (i.e. calculated taking into account the number of hydrogen atoms at each position) relative reactivities of hydrogen atoms in positions 1, 2, 3, and 4 of the hydrocarbon chain, respectively.
[b] PCA is pyrazine-2-carboxylic acid; for this system, see [53].
[c] Mn_2^{IV} is $[LMn^{IV}(O)_3Mn^{IV}L](PF_6)_2$, where L is 1,4,7-trimethyl-1,4,7-triazacyclononane; for this system, see [38,39,54–58].

be seen from the data presented in Tables 7 and 8 that the selectivities for the oxidation catalyzed by $FeCl_3$ in the presence of compound **1** are noticeably higher than that for the reactions without **1**. These results testify that an oxidizing species in the case of the MCPBA–$FeCl_3$–**1** system is more selective than radicals HO· or RO$^\bullet$ and we can conclude that in this reaction neither hydroxyl nor alkoxyl radicals induce the cyclohexane oxidation. This conclusion is supported by the data presented in Fig. 6 which demonstrates that the initial reaction rate is proportional to initial cyclohexane concentration up to 0.8 mol dm^{-3}. It means that only a small portion of formed active species is accepted by the cyclohexane. In oxidations induced by HO$^\bullet$ or RO$^\bullet$ at such high cyclohexane concentration a large portion of all generated active species is accepted with the alkane and the oxidation rate becomes to be independent of the cyclohexane concentration. Such an independence of the reaction rate on cyclohexane concentration at [cyclohexane]$_0$ up to 0.9 mol dm^{-3} was found by us in the oxidation with hydrogen peroxide catalyzed by an iron chloride salt in acetonitrile [59]. In that case a conclusion has been made that an oxidizing species was the Fe(IV) ion. It is reasonable to assume that a system described in the present work oxidizes with the formation of the same ion bound to ligand **1**.

The dependence of the initial reaction rate on initial MCPBA concentration shown in Fig. 5 is in accordance with a proposal about the formation of an adduct, *comp* (see [60–62]), between coordinated with **1** iron ion and the MCPBA molecule [depicted as RC(=O)OOH] which can be a peroxo complex

$$(\mathrm{Fe}\cdot\mathbf{1})^{3+} + \mathrm{RC(=O)OOH} \rightleftharpoons \mathrm{comp} \quad K_2 \tag{2}$$

In accordance with the data of Fig. 5 we can accept that at [MCPBA]$_0 \approx 0.15$ mol dm^{-3} the reaction rate is equal to one half of the maximum rate. Thus concentration of comp is 1/2[(Fe·**1**)$^{3+}$]$_0$ and $K_2 > (0.15)^{-1} \approx 6$ mol^{-1} dm^3.

We propose the following steps in addition to stages (1) and (2):

$$\mathrm{comp} \rightarrow (\mathrm{Fe}\cdot\mathbf{1})^{2+} + \mathrm{RC(=O)OO^\bullet} + \mathrm{H^+} \quad k_3 \tag{3}$$

$$(\mathrm{Fe}\cdot\mathbf{1})^{2+} + \mathrm{RC(=O)OOH} \rightarrow (\mathbf{1}\cdot\mathrm{Fe{=}O})^{4+} + \mathrm{RC(=O)OH} \tag{4}$$

$$(\mathbf{1}\cdot\mathrm{Fe{=}O})^{4+} + \mathrm{CyH} \rightarrow (\mathbf{1}\cdot\mathrm{Fe{-}OH})^{3+} + \mathrm{Cy^\bullet} \tag{5}$$

$$(\mathbf{1}\cdot\mathrm{Fe{=}O})^{4+} + \mathrm{MeCN} \rightarrow \mathrm{products} \tag{6}$$

$$\mathrm{Cy^\bullet} + \mathrm{O_2} \rightarrow \mathrm{CyOO^\bullet} \tag{7}$$

$$\mathrm{CyOO^\bullet} + (\mathrm{Fe}\cdot\mathbf{1})^{2+} + \mathrm{H^+} \rightarrow \mathrm{CyOOH} + (\mathrm{Fe}\cdot\mathbf{1})^{3+} \tag{8}$$

This kinetic model is in accordance also with found linear dependence of the reaction rate on $FeCl_3$ concentration when [$FeCl_3$] < [**1**]. We have to accept in the frames of the proposed mechanism that the rate of the interaction between (**1**·Fe=O)$^{4+}$ and acetonitrile is substantially higher than the rate of the reduction of (**1**·Fe=O)$^{4+}$ with cyclohexane. This statement is based on the data presented in Fig. 6: there is not plateau even at relatively high cyclohexane concentrations (> 0.6 mol dm^{-3}) and the dependence is linear up

Table 8
Stereoselectivity parameters (*trans*/*cis*) in alkane oxidations by various systems in acetonitrile (certain systems are added for comparison), **1**:Fe = 8:1

Entry	System	Substrate[a]					
		cis-1,2-DMCH	*trans*-1,2-DMCH	*cis*-1,4-DMCH	*trans*-1,4-DMCH	*cis*-Decalin	*trans*-Decalin
1	*m*-CPBA–$FeCl_3$	0.7	1.2	2.7	1.3	0.4	0.4
2	*m*-CPBA–$FeCl_3$-**1**	0.25	3.0	0.4	0.75	0.35	0.4
3	*m*-CPBA–complex **3**	0.8	1.5				
4	H_2O_2–*n*-Bu_4NVO_3–PCA[b]	0.75	0.8	1.45	1.6	2.1	2.4
5	H_2O_2–Mn_2^{IV}–MeCOOH[c]	0.35	4.1	0.5	2.2	0.12	33

DMCH, dimethylcyclohexane.
[a] Parameter *trans*/*cis* is the *trans*/*cis* ratio of isomers of *tert*-alcohols formed in the oxidation of *cis*- or *trans*-isomers of DMCH or decalins.
[b] PCA is pyrazine-2-carboxylic acid; for this system, see [53].
[c] Mn_2^{IV} is $[LMn^{IV}(O)_3Mn^{IV}L](PF_6)_2$, where L is 1,4,7-trimethyl-1,4,7-triazacyclononane; for this system, see [38,39,54–58].

to $0.85\,\mathrm{mol\,dm^{-3}}$ of cyclohexane. In this case we can estimate the constant K_3 of the rate of the comp monomolecular decomposition: $k_3[\mathrm{comp}] \gg 0.8 \times 10^{-5}\,\mathrm{mol\,dm^{-3}\,s^{-1}}$ and $k_3 \gg (0.8 \times 10^{-5})/(2 \times 10^{-4}) = 0.04\,\mathrm{s^{-1}}$. It is interesting that this value is much higher than the rate constant for the monomolecular decomposition of a peroxo iron(III) complex in water.

4. Conclusion

This work demonstrates that the addition to a metal-complex catalyst a polydentate amine (which mimics a peptide environment of a reaction center in an enzyme) leads to a great enhancement of the alkane oxidation rate as well as selectivity of the reaction.

Acknowledgements

We thank the Russian Basic Research Foundation and the State of São Paulo Research Foundation (Fundação de Amparo a Pesquisa do Estado de São Paulo, FAPESP), the Brazilian National Council on Scientific and Technological Development (Conselho Nacional de Desenvolvimento Cientifico e Tecnológico, CNPq, Brazil) for support. This work was also supported by the grant from the Section of Chemistry and Material Science of the Russian Academy of Sciences (Program “A theoretical and experimental study of chemical bonds and mechanisms of main chemical processes”, Project “The solvent effects in redox processes that include the electron transfer stages”).

G.B. Shul’pin expresses his gratitude to the FAPESP (grant no. 2002/08495-4), the CNPq (grant no. 300601/01-8), the Faculdade de Química, Pontifícia Universidade Católica de Campinas and the Instituto de Química, Universidade Estadual de Campinas for making it possible for him to stay at these Universities as invited Professor and to perform a part of the present work.

References

[1] A.E. Shilov, G.B. Shul’pin, Chem. Rev. 97 (1997) 2879–2932.
[2] P.E.M. Siegbahn, R.H. Crabtree, J. Am. Chem. Soc. 119 (1997) 3103–3113.
[3] K. Yoshizawa, T. Ohta, T. Yamabe, R. Hoffmann, J. Am. Chem. Soc. 119 (1997) 12311–12321.
[4] E.K. van der Beuken, B.L. Feringa, Tetrahedron 54 (1998) 12985–13011.
[5] M. Fontecave, S. Ménage, C. Duboc-Toia, Coord. Chem. Rev. 178–180 (1998) 1555–1572.
[6] J.-P. Willems, A.M. Valentine, R. Gurbiel, S.J. Lippard, B.M. Hoffman, J. Am. Chem. Soc. 120 (1998) 9410–9416.
[7] R.J. Deeth, H. Dalton, JBIC 3 (1998) 302–306.
[8] A.M. Valentine, S.S. Stahl, S.J. Lippard, J. Am. Chem. Soc. 121 (1999) 3876–3887.
[9] A.E. Shilov, G.B. Shul’pin, Oxidation in living cells and its chemical models, Activation and Catalytic Reactions of Saturated Hydrocarbons in the Presence of Metal Complexes, Kluwer Academic Publishers, Dordrecht/Boston/London, 2000, chapter XI, pp. 466–522.
[10] M. Costas, K. Chen, L. Que Jr., Coord. Chem. Rev. 200–202 (2000) 517–544.
[11] E.I. Solomon, T.C. Brunold, M.I. Davis, J.N. Kemsley, S.-K. Lee, N. Lehnert, F. Neese, A.J. Skulan, Y.-S. Yang, J. Zhou, Chem. Rev. 100 (2000) 235–349.
[12] D. Lee, S.J. Lippard, Inorg. Chem. 41 (2002) 827–837.
[13] R.A. Friesner, M.-H. Baik, B.F. Gherman, V. Guallar, M. Wirstam, R.B. Murphy, S.J. Lippard, Coord. Chem. Rev. 238–239 (2003) 267–290.
[14] A. Bassan, M.R.A. Blomberg, P.E.M. Siegbahn, Chem. Eur. J. 9 (2003) 4055–4067.
[15] M.-H. Baik, M. Newcomb, R.A. Friesner, S.J. Lippard, Chem. Rev. 103 (2003) 2385–2419.
[16] S. Ito, T. Okuno, H. Itoh, S. Ohba, H. Matsushima, T. Tokii, Y. Nishida, Z. Naturforsch. 52b (1997) 719–727.
[17] P.P. Knops-Gerrits, S. Dick, A. Weiss, M. Genet, P. Rouxhet, X.Y. Li, P.A. Jacobs, in: R.K. Grasselli, S.T. Oyama, A.M. Gaffney, J.E. Lyons (Eds.), Third World Congress on Oxidation Catalysis, Elsevier, Amsterdam, 1997, pp. 1061–1070.
[18] C. Duboc-Toia, S. Ménage, C. Lambeaux, M. Fontecave, Tetrahedron Lett. 38 (1997) 3727–3730.
[19] S. Ménage, J.-B. Galey, J. Dumats, G. Hussler, M. Seité, I.G. Luneau, G. Chottard, M. Fontecave, J. Am. Chem. Soc. 120 (1998) 13370–13382.
[20] S. Nishino, H. Hosomi, S. Ohba, H. Matsushima, T. Tokii, Y. Nishida, J. Chem. Soc., Dalton Trans. (1999) 1509–1513.
[21] G. Roelfes, M. Lubben, R. Hage, L. Que Jr., B.L. Feringa, Chem. Eur. J. 6 (2000) 2152–2159.
[22] G.V. Nizova, B. Krebs, G. Süss-Fink, S. Schindler, L. Westerheide, L. Gonzalez Cuervo, G.B. Shul’pin, Tetrahedron 58 (2002) 9231–9237.
[23] G. Roelfes, V. Vrajmasu, K. Chen, R.Y.N. Ho, J.-U. Rohde, C. Zondervan, R.M. la Crois, E.P. Schudde, M. Lutz, A.L. Spek, R. Hage, B.L. Feringa, E. Münk, L. Que Jr., Inorg. Chem. 42 (2003) 2639–2653.
[24] V. Balland, F. Banse, E. Anxolabéhère-Mallart, M. Nierlich, J.-J. Girerd, Eur. J. Inorg. Chem. (2003) 2529–2535.
[25] É. Balogh-Hergovich, G. Speier, M. Réglier, M. Giorgi, E. Kuzmann, A. Vértes, Eur. J. Inorg. Chem. (2003) 1735-1740.
[26] P.-P.H.J.M. Knops-Gerrits, W.A. Goddard III, Catal. Today 81 (2003) 263–286.
[27] J. Kaizer, M. Costas, L. Que Jr., Angew. Chem. Int. Ed. 42 (2003) 3671–3673.
[28] H. Furutachi, M. Murayama, A. Shiohara, S. Yamazaki, S. Fujinami, A. Uehara, M. Suzuki, S. Ogo, Y. Watanabe, Y. Maeda, Chem. Commun. (2003) 1900–1901.
[29] M.P. Jensen, S.J. Lange, M.P. Mehn, E.L. Que, L. Que Jr., J. Am. Chem. Soc. 125 (2003) 2113–7842.
[30] T.L. Foster, J.P. Caradonna, J. Am. Chem. Soc. 125 (2003) 3678–3679.
[31] M.P. Mehn, K. Fujisawa, E.L. Hegg, L. Que Jr., J. Am. Chem. Soc. 125 (2003) 7828–7842.
[32] M. Fujita, M. Costas, L. Que Jr., J. Am. Chem. Soc. 125 (2003) 9912–9913.
[33] M. Kodera, H. Shimakoshi, K. Kano, Chem. Commun. (1996) 1737–1738.
[34] W. Nam, J.Y. Ryu, I. Kim, C. Kim, Tetrahedron Lett. 43 (2002) 5487–5490.
[35] M. Yamaguchi, H. Kousaka, T. Yamagishi, Chem. Lett. (1997) 769–770.
[36] K. Jitsukawa, Y. Oka, H. Einaga, H. Masuda, Tetrahedron Lett. 42 (2001) 3467–3469.
[37] M. Yamaguchi, Y. Ichii, S. Kosaka, D. Masui, T. Yamagishi, Chem. Lett. (2002) 434–435.

[38] J.R. Lindsay Smith, G.B. Shul'pin, Tetrahedron Lett. 39 (1998) 4909–4912.
[39] G.B. Shul'pin, J.R. Lindsay Smith, Russ. Chem. Bull. 47 (1998) 2379–2386.
[40] G.B. Shul'pin, J. Mol. Catal. A: Chem. 189 (2002) 39–66.
[41] G.B. Shul'pin, Comptes Rendus – Chimie 6 (2003) 163–178.
[42] G.M. Sheldrick, SHELXS-97, Program for the Solution of Crystal Structures, Acta Crystallogr. A46 (1990) 467.
[43] G.M. Sheldrick, SHELXL-97, Program for the Refinement of Crystal Structures, University of Göttingen, Germany, 1997.
[44] A.L. Spek, Acta Crystallogr. A46 (1990) C34.
[45] E. Keller, Schakal 97, A Computer Program for the Graphic Representation of Molecular and Crystallographic Models, University of Freiburg, Germany, 1997.
[46] A. Tesouro Vallina, H. Stoeckli-Evans, Acta Crystallogr. C57 (2001) 489–490.
[47] G.B. Shul'pin, A.N. Druzhinina, React. Kinet. Catal. Lett. 48 (1992) 333–338.
[48] G.B. Shul'pin, G.V. Nizova, React. Kinet. Catal. Lett. 47 (1992) 207–211.
[49] G.B. Shul'pin, D. Attanasio, L. Suber, J. Catal. 142 (1993) 147–152.
[50] G.B. Shul'pin, M.M. Bochkova, G.V. Nizova, J. Chem. Soc., Perkin Trans. 2 (1995) 1465–1469.
[51] G.B. Shul'pin, G.V. Nizova, Yu.N. Kozlov, New J. Chem. 20 (1996) 1243–1256.
[52] G.B. Shul'pin, Alkane oxidation: estimation of alkyl hydroperoxide content by GC analysis of the reaction solution samples before and after reduction with triphenylphosphine, The Chemistry Preprint Server, http://preprint.chemweb.com/orgchem/0106001, 2001, pp. 1–6.
[53] G.B. Shul'pin, Yu.N. Kozlov, G.V. Nizova, G. Süss-Fink, S. Stanislas, A. Kitaygorodskiy, V.S. Kulikova, J. Chem. Soc., Perkin Trans. 2 (2001) 1351–1371.
[54] G.B. Shul'pin, G. Süss-Fink, J.R. Lindsay Smith, Tetrahedron 55 (1999) 5345–5358.
[55] G.B. Shul'pin, G. Süss-Fink, L.S. Shul'pina, J. Mol. Catal. A 170 (2001) 17–34.
[56] G.B. Shul'pin, Petrol. Chem. 41 (2001) 405–413.
[57] G.B. Shul'pin, G.V. Nizova, Yu.N. Kozlov, I.G. Pechenkina, New J. Chem. 26 (2002) 1238–1245.
[58] G.V. Nizova, C. Bolm, S. Ceccarelli, C. Pavan, G.B. Shul'pin, Adv. Synth. Catal. 344 (2002) 899–905.
[59] G.B. Shul'pin, G.V. Nizova, Yu.N. Kozlov, L. Gonzalez Cuervo, G. Süss-Fink, Adv. Synth. Catal. 346 (2004) 317–332.
[60] G.B. Shul'pin, Yu.N. Kozlov, Org. Biomol. Chem. 1 (2003) 2303–2306.
[61] G.B. Shul'pin, J. Gradinaru, Yu.N. Kozlov, Org. Biomol. Chem. 1 (2003) 3611–3617.
[62] L. Gonzalez Cuervo, Yu.N. Kozlov, G. Süss-Fink, G.B. Shul'pin, J. Mol. Catal. A: Chem. 218 (2004) 171–177.